PHYSICAL REVIEW B **72**, 195108 (2005)

Analysis of the thermal behavior of photoluminescent optical memory based on CaS:Eu,Sm media

C. Chen,[1] K. L. Teo,[1,*] T. C. Chong,[1] D. M. Newman,[2] and J. P. Wu[3]
[1]*Information Storage Materials Laboratory, Department of Electrical and Computer Engineering, National University of Singapore, 4 Engineering Drive 3, Singapore 117576 and Data Storage Institute, 5, Engineering Drive 1, Singapore 117608*
[2]*School of Engineering Computer Science and Mathematics, University of Exeter, Exeter EX4 4QF, United Kingdom*
[3]*Department of Engineering, Queen Mary College, University of London, London, United Kingdom*
(Received 31 March 2005; revised manuscript received 27 September 2005; published 17 November 2005)

The temperature dependence of the photoluminescence (PL) and infrared stimulated luminescence (ISL) exhibited by CaS doped with both europium (Eu) and samarium (Sm) ions is reported for temperatures in the range between 100 and 700 K. Behavior indicative of strong electron-phonon coupling is observed in the PL emission of the Eu^{2+} ion and two processes with activation energies $(\Delta E_1, \Delta E_2)$ are recognized in the quenching of the PL intensity. The smaller of these $(\Delta E_2 = 0.056\ \mathrm{eV})$ is identified as the energy separation between Eu^{2+} excited states and the conduction band of CaS while ΔE_1, which has a value of 0.55 eV, is attributed to some intervening quenching state. On the other hand, analysis of the integrated ISL intensity as a function of temperature prompts the conclusion that the separation $(\Delta\varepsilon)$ between the lowest excited energy levels of Eu^{2+} ions and that of Sm^{2+} ions is approximately 28 meV at low temperature. When it is considered for an optical memory medium, recording experiments performed at different temperatures show the writing process to be more efficient when conducted at higher temperatures rather than lower ones. Moreover, two different time constants, that are themselves linear functions of temperature, are observed to govern the readout process in which electrons trapped at the Sm ions are depleted under continuous (IR) irradiation. Finally, studies of the ISL intensity versus storage time at different temperatures show the reading output to be lowered for longer storage times due to a thermally assisted decay route facilitating the release of electrons trapped at Sm^{2+} ions back to Eu^{2+} ions.

DOI: 10.1103/PhysRevB.72.195108 PACS number(s): 78.55.Et, 78.66.Hf, 71.55.Gs

I. INTRODUCTION

Electron trapping optical materials (ETOM) formed by doping compounds such as strontium or calcium sulfide (SrS, CaS) with both Eu and Sm exhibit infrared stimulated luminescence (ISL) at room temperature following excitation with either visible or ultraviolet (UV) radiation.[1–3] Material systems such as SrS:Eu,Sm and CaS:Eu,Sm are consequently considered good candidate media for the development of optical memory technology based on nonthermal recording processes. The adoption of ETOM offers many advantages[4–6] over the thermal processes employed in all currently commercialized forms of optical recording. Of the two systems CaS:Eu,Sm shows a more rapid time response,[7] it is more chemically stable[8] and is hence selected as the basis of our investigation.

In the optical recording process envisioned for material systems of this type, the Eu and Sm ions form activation and trapping centers, respectively. Storing data ("writing") into these materials is accomplished through ionization of a Eu center $(Eu^{2+} \rightarrow Eu^{3+} + e^-)$ with the subsequent capture of the ejected electron by a Sm trapping center $(Sm^{3+} + e^- \rightarrow Sm^{2+})$. "Readout" occurs by what is essentially the reverse of this procedure and further exploits the ISL phenomena. The electrons trapped at the Sm center are excited $(Sm^{2+} \rightarrow Sm^{3+} + e^-)$ by infrared radiation and ultimately transfer to and recombine with an Eu center $(Eu^{3+} + e^- \rightarrow Eu^{2+})$, signifying completion of this process by the emission of radiation at around 650 nm. If the overall charge transfer reaction for these processes is written $(Eu^{2+} + Sm^{3+} \Leftrightarrow Eu^{3+} + Sm^{2+})$, the reaction is then driven to the right by visible/uv light excitation in the "write" band and to the left by IR excitation in the "read" band.[9–12]

It is well known that the Eu^{2+} and Sm^{3+} ions have very different optical emission characteristics. The Eu^{2+} ion displays a broad emission band arising from transitions between the $4f^7$-$4f^6 5d^1$ states[13,14] which can be observed under either visible or UV excitation. In contrast, emission from Sm^{3+} is characterized by a series of sharp lines from the $^4G_{5/2}$-$^6H_{5/2}$, $^6H_{9/2}$, and $^6H_{11/2}$ states, which can only be observed with UV excitation.[15]

In many divalent rare-earth ions in crystals such as Eu^{2+} in SrS (Refs. 13 and 16) and Sm^{2+} in SrS,[17] optical transitions between the states $(4f^{n-1}5d \rightarrow 4f^n)$ generally show strong electron-phonon coupling. In the present study, the temperature dependence of photoluminescence (PL) from CaS:Eu,Sm is measured between 100 and 700 K and the results are analyzed in terms of an electron-phonon coupling model using a one-dimensional configuration coordinate diagram. It is found that the optically active excitation states of $4f^6 5d^1$ of Eu^{2+} in CaS are strongly coupled to the lattice vibrational modes. We propose that the observed quenching of the PL intensity occurs via some intervening quenching state, which is consistent with our previous high-pressure studies.[18]

Thermoluminescence (TL),[9,10,19–22] infrared-stimulated luminescence (ISL),[7] and photoconductivity[16] are useful techniques for the determination of the trapping processes in many alkali-earth sulfide materials. Although the ISL characteristics of alkali-earth sulfide materials are well documented,[4–7,9–11,23–33] there have been no systematic studies of ISL as a function of temperature in these materials. In the present study, the read-write experiment is performed at different temperatures and the ISL spectra are measured between 100 and 700 K. It is found that is is more efficient to write at high temperatures than at lower ones, but the reading efficiency does not depend very much on temperature. It is inferred that the lowest excited energy level of Eu^{2+} is lower than that of Sm^{2+} by ~28 meV. In addition; we have also performed the experiment to study the depletion rate of trapped electrons under constant IR irradiation as a function of temperature over the range of 150 to 400 K. The decay of ISL intensity is fitted using two time constants. Furthermore, the ISL output at the single wavelength of 650 nm as a function of storage time was measured at different temperatures The results show that the output is only a very weak function of storage time at low temperature. At higher temperature, however, the detrapping rate is higher due to the fact that the electrons trapped at Sm centers are detrapped with the assistance of thermal energy. An improved understanding of the energy levels diagram in CaS:Eu,Sm is made possible by an analysis of all these results.

II. EXPERIMENT

The samples investigated were formed using calcium sulfide powder (Aldrich 99.99%) mixed intimately with concentrations of Eu_2O_3 (99.99%) and Sm (99.99%) together with 0.1% weight of elemental sulfur to provide a sulfurizing atmosphere during initial heating. The dopant concentrations are 1000 p and 750 ppm for Eu and Sm, respectively. These concentrations have been previously reported as the optimum to obtain maximum ISL emission.[30] The mixture was heated in a tube furnace at 1200 °C for 2 h under nitrogen atmosphere. The full details of the preparation technique are given in Ref. 6. For optical characterization of this material, the 488 nm Ar^+ ion laser line was used as the visible-light source for writing the information and the ISL emission were stimulated with a laser diode at 1064 or 980 nm. The laser power intensity is kept at 1 mW/cm^2 for both visible and IR light sources as to prevent laser-induced heating. Both PL and ISL emissions are analyzed with a TRIAX550 spectrometer coupled to a photomultiplier tube (PMT) using a standard lock-in amplifier technique. For temperature dependence measurements, the sample is mounted on a sample holder in a cryostat. Temperature was varied from 100 to 700 K.

III. RESULTS AND DISCUSSION

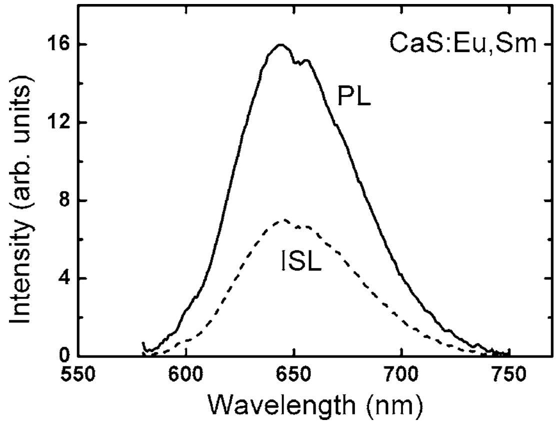

FIG. 1. PL and ISL spectra of CaS:Eu,Sm at 300 K.

Figure 1 shows a typical PL and ISL spectra of CaS:Eu,Sm at 300 K. The PL spectrum is taken by exciting the sample only with Ar^+ ion laser light at 488 nm while the ISL spectrum is obtained when CaS:Eu,Sm is stimulated with infrared light at 1064 nm after prior irradiation with 488 mn laser light. Both spectra are peaked at around 650 nm as expected due to 4f–5d transition in Eu^{2+} ions. The temperature dependence of the integrated intensity of the PL peak energy between 100 and 700 K is shown in Fig. 2(a) with the measurement conducted in two cycles (upstroke and downstroke). Similarly, Figs. 2(b) and 2(c) show, respectively, the PL peak energy and the full-width at half maximum (FWHM) obtained from the PL emission spectra between 100 and 700 K. It is observed that the integrated intensity decreases while the peak energy and the FWHM both increase with increasing temperature. The observed decrease in intensity with temperature is best fitted to the experimental data using a function that describes the observed behavior as arising from two thermally activated quenching processes,

$$I_{PL}(T) = \frac{I(0)}{1 + A_1 \exp\left(\frac{-\Delta E_1}{k_B T}\right) + A_2 \exp\left(\frac{-\Delta E_2}{k_B T}\right)}, \tag{1}$$

where $I(0)=8002\pm104$, $A_1=39\,034\pm42$ and $\Delta E_1=0.55\pm0.06$ eV, $A_2=4.63\pm0.46$ and $\Delta E_2=0.056\pm0.003$ eV. Attempts to fit the data to a function using only single activation energy gave considerably poorer results and greater fitting errors. The increase in the PL peak energy as a function of temperature can be fitted quadratically as follows:

$$E_{PL}(T) = E_{PL}(0) + E_1 T + E_2 T^2, \tag{2}$$

where $E_{PL}(0)=1.894\pm0.001$ eV, $E_1=(8.63\pm0.61)\times10^{-5}$ eV/K, and $E_2=(1.07\pm0.07)\times10^{-7}$ eV/K^2.

As previously indicated, the optical transitions ($4f^{n-1}5d \rightarrow 4f^n$) for many divalent rare-earth ions in crystals generally show strong electron-phonon coupling.[7] The line shape and temperature dependence of the PL spectra are thus further analyzed using an electron-phonon coupling model with one-dimensional "configuration coordinate" (c.c.) diagram as shown in Fig. 3. The energy of the coupled phonon Ω may be obtained from the temperature dependence of the FWHM, $W(T)$ equation as follows[34]

$$W(T) = W(0)\left\{\tanh\left(\frac{\Omega}{2k_B T}\right)\right\}^{-0.5}. \tag{3}$$

Fitting Eq. (3) to the experimental $W(T)$ data gives $W(0)=0.103\pm0.003$ eV and $\Omega=0.021\pm0.001$ eV as best fitted values. The result is shown as a solid line in Fig. 2(c). These values are in close correspondence with the values of 0.15 and 0.02 eV recorded for these parameters in SrS:Eu,Sm.[17]

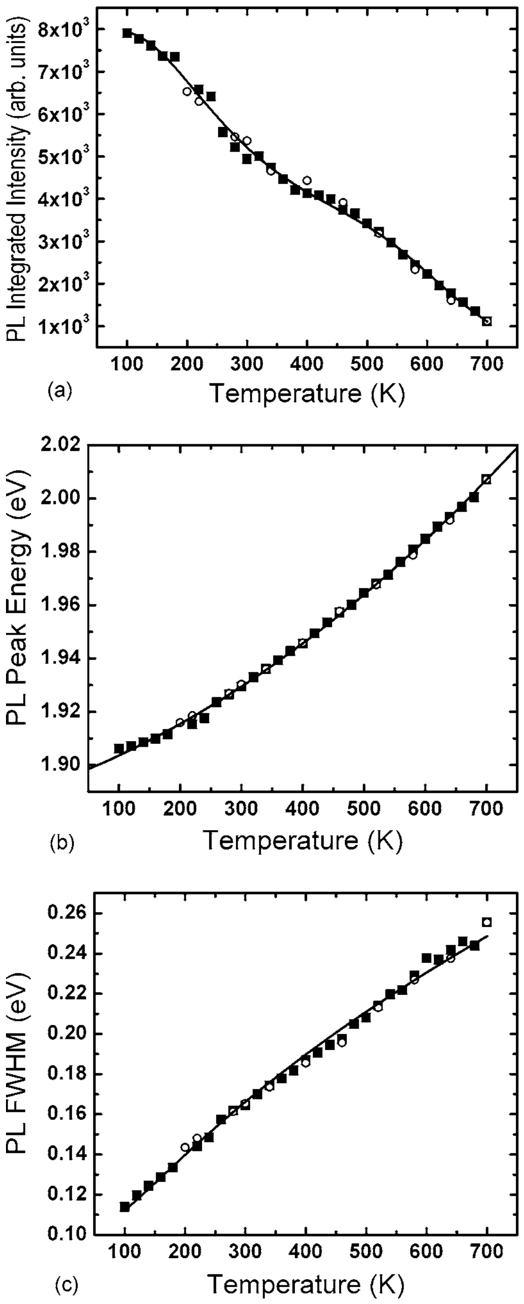

FIG. 2. (a) PL integrated intensity as a function of temperature. The solid squares are for the upstroke temperature cycle (100 to 700 K); the open circles are for the down-stroke temperature cycle (700 to 100 K). The solid line is the fitted result. (b) PL peak energy as a function of temperature. The solid squares are for the upstroke temperature cycle (100 to 700 K); the open circles are for the down-stroke temperature cycle (700 to 100 K). The solid line is the fitted result. (c) FWHM of PL as a function of temperature. The solid squares are for the upstroke temperature cycle (100 to 700 K); the open circles are for the down-stroke temperature cycle (700 to 100 K). The solid line is the fitted result.

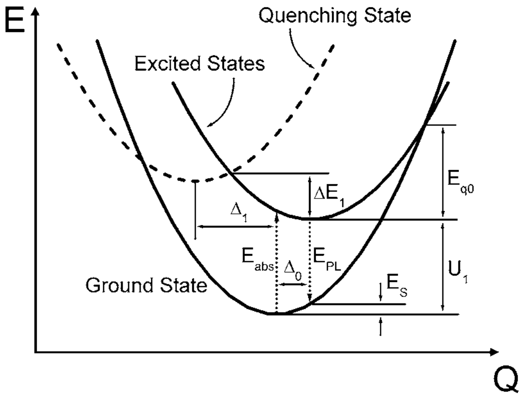

FIG. 3. The schematic configuration coordinate diagram for Eu^{2+} ions in CaS:Eu,Sm. Δ_0 is the relative displacement of the excited state potential well with respect to the ground state; E_{PL} is the PL emission energy; E_{abs} is the absorption energy; U_1 is the electronic energy difference between the minimum points of ground and excited states of the Eu^{2+} ions; E_S is the Stokes shift ($U_1 - E_{PL}$); E_{q0} is the energy barrier for an electron to cross over nonradiatively to the equilibrium of the excited potential well; ΔE_1 is the activation energy for the electron to cross over to the quenching state.

Another important parameter of the electron-phonon coupling model is the Stokes shift (E_S). If the coupled phonon energy Ω and $W(0)$ are known, the Stokes shift is given by

$$E_S = \frac{[W(0)]^2}{8\Omega \ln 2}. \tag{4}$$

Substituting $W(0)=0.103$ eV and $\Omega=0.021$ eV, as obtained in Eq. (3), into Eq. (4) yields $E_S=0.091\pm0.007$ eV.

We have rewritten Eq. (2) in terms of zero-phonon energy and the Stokes shift (E_S) which gives

$$E_{PL}(T) = U(T) - E_S, \tag{5}$$

where $U(T)$ is the electronic energy difference between the minimum points of ground and excited states of the Eu^{2+} ions. Substituting the values determined for $E_{PL}(0) = 1.894$ eV and $E_S=0.091$ eV gives $U(0)=1.985\pm0.008$ eV.

Another important parameter that can be obtained from the model is the electron-phonon coupling strength (S), which is representative of the average number of phonons created during lattice relaxation after an electronic transition

$$S = \frac{E_S}{\Omega} = \frac{[W(0)]^2}{8\Omega^2 \ln 2}. \tag{6}$$

Inserting values already determined for $W(0)$ and Ω gives a reasonably large $S=4.3\pm0.7$ value for the coupling strength. In contrast to crystals of a more ionic nature doped with Eu^{2+},[35] the zero-phonon line is too weak to be observed in CaS doped with Eu^{2+}.

The model also predicts the absorption transition energy, $E_{abs}(T)$. Since all the dependent variables are now known, this too can be calculated at any temperature. Using

$$E_{abs}(T) = U(T) + E_s = E_{PL}(T) + 2E_s \tag{7}$$

shows $E_{abs}(0)=2.076\pm0.015$ eV at 0 K increasing to $E_{abs}(300)=2.112\pm0.017$ eV at room temperature (300 K).

We note that the PL emission of Eu^{2+} ions originates from the crystal field splitting of the Eu atomic energy levels by the lattice. The atomic separation increases with temperature, weakening the effect of the crystal field splitting that one would expect to produce a blueshift in the emission peak. However, this effect is small since the change in lattice constants due to thermal expansion is small. On the other hand, since the population of the excited states is strongly dependent on temperature, any increase in temperature will cause more excited states, i.e., vibronic states to be populated. This leads to both a shift and broadening of the emission peak.[36] As shown in the configuration coordinate diagram of Fig. 3, the quenching energy E_{qo} describes the potential required for an electron to cross over nonradiatively to the ground state potential well. This energy is given by

$$E_{qo} = \frac{[U(0) - E_S]^2}{4E_S}, \tag{8}$$

which yields a value of $E_{q0}=9.86\pm0.77$ eV, as compared to the value of 7.04 ± 0.76 eV determined for E_{q0} at one atmospheric pressure in our previous high pressure studies[18] on CaS:Eu^{2+}. Although the values obtained from two different experiments do not exactly agree, they are of the same order of magnitude. We note that the observed activation energies $\Delta E_1=0.55$ eV and $\Delta E_2=0.056$ eV obtained from Eq. (1) are much smaller than the E_{q0} value. The quenching of PL with activation energy $\Delta E_1=0.55$ eV is thought to most likely occur via some intervening quenching state with a large Δ_1 value as shown in Fig. 3 and which again was successfully invoked when modeling our previous high pressure results.[18] The other PL quenching activation energy $\Delta E_2=0.056$ eV corresponds closely to the observed energy gap between Eu^{2+} excited states and the conduction band of host material CaS.[13] In CaS, the valence-band maximum (VBM) is at the Γ point and the conduction-band minimum (CBM) is at the X point. The indirect gap is 4.3 eV. The direct gap is 5.8 eV, which is the energy separation between VBM and the CBM; both located at the Γ point. The energy separation between the excited state of Eu^{2+} and the CBM at the X point is $\Delta E_2=0.056$ eV as proposed in our model. On the other hand, the trapping state, corresponding to $\Delta E_1=0.55$ eV, lies below the CBM at the Γ point but above the CBM at the X point with respect to the Eu^{2+} excited states. Electrons transit between the electronic states of the same ion with higher efficiency than between impurity ions and the band. For example, in Fig. 2 of Ref. 27, the absorption peak is observed for 4*f*–5*d* transition, in which an electron transits from Eu^{2+} ground state to its excited state above the CBM at the X point of CaS. However, the electronic transition between impurity ion and the band is not observed. This suggests that the Eu^{2+} trapping states above the CBM at the X points can trap electrons easily from other Eu^{2+} states.

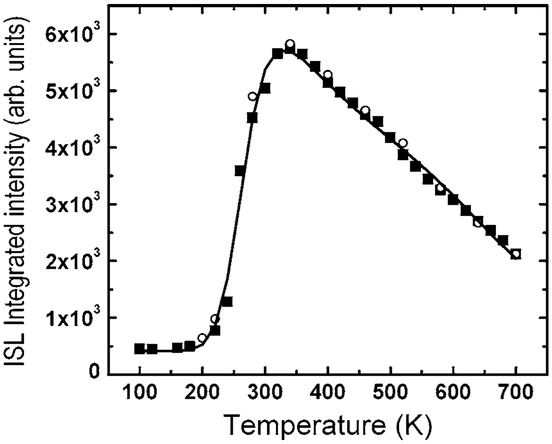

FIG. 4. ISL integrated intensity as a function of temperature. The solid squares are for the upstroke temperature cycle (100 to 700 K); the open circles are for the down-stroke temperature cycle (700 to 100 K). The solid line is a guide to the eye.

Figure 4 shows the integrated intensity of ISL as a function of temperature. At each temperature, the integrated intensity is obtained from the ISL spectra by stimulating the samples with IR light after visible irradiation for 1 min. When the samples are first exposed to the blue light, the 4*f*–5*d* transitions of Eu^{2+} ions occur. In addition to the electrons relaxing to the ground state, some of the electrons are transferred to the 5*d* excited state of Sm^{2+} ions by thermally assisted tunneling processes, and subsequently the electrons relax to the Sm^{2+} ground state. We note that the visible light excitation is at 488 nm (2.541 eV) from an Ar$^+$ ion laser. This level of energy cannot provide a transition from the Eu^{2+} ground state to the conduction band and therefore no photoelectrons can be produced in the conduction band. When stimulated with IR light, in addition to the electron relaxing to the ground state, some of the electrons left are transferred to the 5*d* excited state of Eu^{2+} ions and give rise to the radiation of 5*d*–4*f* transition of Eu^{2+} ions. Figure 4 shows the ISL integrated intensity increases with temperature and reaches an optimum value at 320 K. Thereafter, the intensity decreases with temperature. We have fitted the intensity curve to a thermally activated quenching process for the temperature range between 320 and 700 K,

$$I_{ISL}(T) = \frac{I(0)}{\left[1 + A_1 \exp\left(\frac{-\Delta E_3}{k_B T}\right)\right]}. \tag{9}$$

The best fit of Eq. (9) to the data gives $I(0)=5471\pm71$, $A_1=71.8\pm9.3$, and $\Delta E_3=0.22\pm0.01$ eV. The activation energy ΔE_3 is attributed to some nonradiative mechanisms that control the quenching of ISL intensity.

In order to understand the increase of ISL intensity in the low temperature range $100\leqslant T\leqslant 300$ K, a recording experiment is performed at different temperatures. For writing, the sample is excited with blue light for 1 min to saturate the Sm^{2+} trapped electron population, while for readout the sample is excited with IR light after the blue light is blocked. The ISL readout intensity is then obtained by measuring the emission at 650 nm under constant IR-light exposure, a phenomenon known as depletion. The results obtained are shown in Fig. 5. In Figs. 5(a) and 5(b), the reading output appears to remain unchanged between 100 and 300 K after the writing, being carried out at $T=100$ K in both cases. Similarly, in Figs. 5(c) and 5(d), the reading output also remains relatively unchanged between 100 and 300 K after the writing is done at $T=300$ K in both cases. However, the reading output is a factor 5 stronger in Figs. 5(c) and 5(d) as compared to Figs. 5(a) and 5(b). This implies that it is more

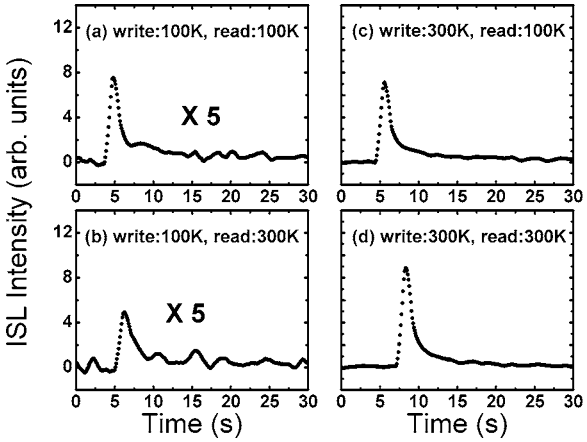

FIG. 5. Depletion curves of trapped electrons with reading and writing at different temperatures.

efficient to write at higher rather than lower temperature, which in turn affects the readout intensity. We conclude that at low temperature it is difficult for electrons to tunnel from Eu^{2+} excited states to Sm^{2+} excited states upon writing and therefore fewer electrons are eventually stored in the Sm^{2+} ground state. Subsequently, during readout, fewer electrons will be transferred back to the Eu^{3+} ions from Sm^{2+} ions resulting in the observed decrease of the emission intensity from the Eu^{2+} ions. It is inferred that the lowest excited energy level of Sm^{2+} ions is higher than that of Eu^{2+} ions and this results in less overlap between the excited energy levels of the two ions thereby reducing the efficient transfer between them. Thus, at low temperature, electrons can easily tunnel from the lowest excited energy level of Sm^{2+} ions to that of Eu^{2+} ions with little thermal assistance, but not vice versa. With increasing temperature, the transfer probability becomes higher since the excited energy levels of Eu^{2+} are in resonance with that of Sm^{2+} ions due to thermal assistance given to tunneling electrons. In Fig. 4, the ISL integrated intensity is seen to peak at 320 K, which is equivalent to $kT \sim 28$ meV. It is deduced that the separation between the lowest excited energy levels of Eu^{2+} ions and Sm^{2+} ions is approximately $\Delta\varepsilon \sim 28$ meV as shown in Fig. 6. Thus, thermal assistance is necessary for efficient writing.

Figure 7 shows the depletion curves of ISL intensity measured at 650 nm under constant IR-light exposure at different temperatures. The solid lines are fits to the IR depletion curves using two time constants in the following equation:

$$I_{ISL}(t) = C + A_1 \exp\left(-\frac{t}{\tau_1}\right) + A_2 \exp\left(-\frac{t}{\tau_2}\right). \qquad (10)$$

Figures 8(a) and 8(b) show these time constants τ_1 and τ_2 are themselves functions of temperature. Values obtained by least-square fittings are

$$\tau_1 = 0.125 + 2.8 \times 10^{-3}\ \mathrm{T},$$

$$\tau_2 = 3.18 + 14 \times 10^{-3}\ \mathrm{T}. \qquad (11)$$

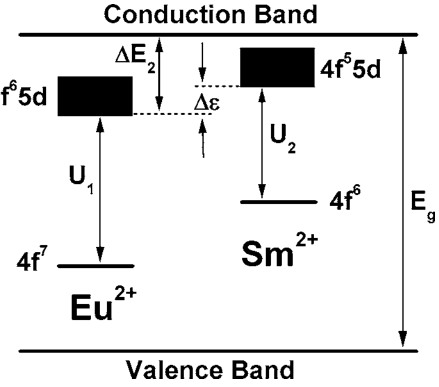

FIG. 6. Energy levels diagram of CaS:Eu, Sm. E_g=4.3 eV (from Ref. 36); U_1=1.985 eV [obtained from Eq. (5)]; U_2=0.942 eV (from Ref. 15); ΔE_2=0.056 eV [obtained from Eq. (1)] and $\Delta\varepsilon$ =28 meV [obtained from Fig. 4].

We see that both τ_1 and τ_2 increase linearly with temperature. These results are explained using a simple model in which P^r_{Sm} and P^{nr}_{Sm} are defined as the probabilities of electrons in excited states of the Sm^{2+} ion returning to the ground state of the Sm^{2+} ion by radiative and nonradiative processes, respectively. Similarly, the probability of electrons tunneling from the excited energy levels of Sm^{2+} ions to Eu^{2+} ions is defined by $P_{Sm\to Eu}$. Of course, $P_{Sm\to Eu}$ is a function of the distance between Eu and Sm ions. On the other hand, the temperature also influences $P_{Sm\to Eu}$. It has been predicted that incorporation of Sm^{2+} ions in a host crystal such as SrS:Eu,Sm, produces strong electron-phonon coupling,[17] implying that P^{nr}_{Sm}

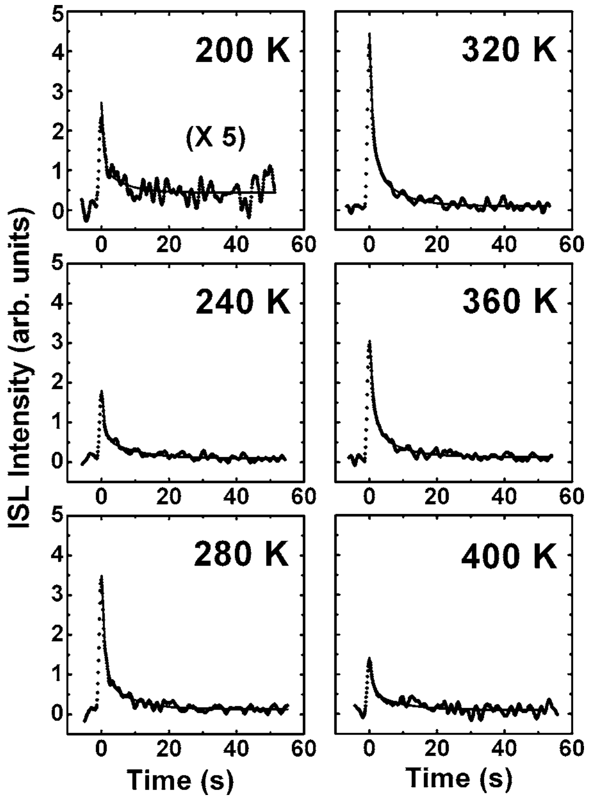

FIG. 7. The depletion curves of trapped electrons under constant IR-light exposure at different temperature. The solid lines are fitted according to Eq. (10).

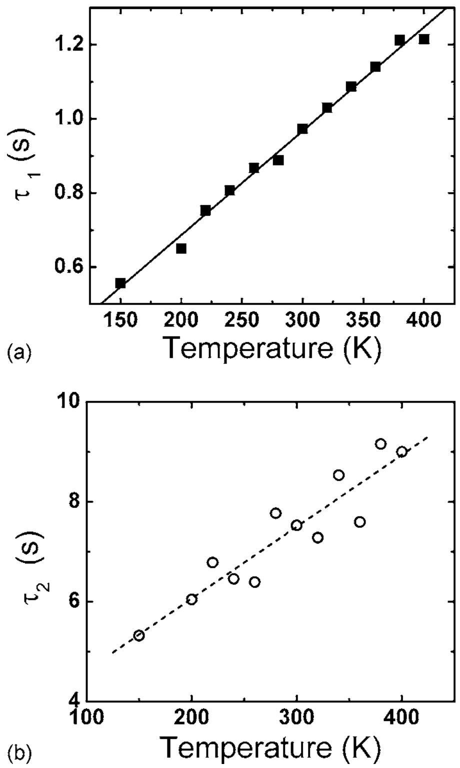

FIG. 8. (a) τ_1 and (b) τ_2 as functions of temperature.

$\gg P^r_{Sm}$. It is worth noting that P^{nr}_{Sm} also increases with increasing temperature. During the readout process, the IR light intensity is kept constant so that it is reasonable to assume that the rate of exciting the electrons from Sm^{2+} ground states to its excited state also remains constant. On the other hand, the total recombination process $(1/\tau_T = 1/\tau_r + 1/\tau_{nr})$ increases with temperature due to the increase in the nonradiative recombination process. Thus at higher temperatures, the ratio of the number of electrons at the Sm^{2+} excited state over the number of electrons at its ground state is much less. Consequently, the rate at which electrons are transferred from the excited energy levels of Sm^{2+} ions to Eu^{2+} ions will also decrease at higher temperature. Thus, it takes longer for electrons trapped at Sm ions to be depleted under IR irradiation resulting in an increase in both τ_1 and τ_2 with temperature. The different time constants τ_1 and τ_2 may originate from different nonradiative mechanisms.

Figures 9(a) and 9(b) show logarithmic plots of ISL reading output versus storage time at different temperatures ranging from 150 to 400 K. The ISL reading output is the area under the depletion curve as shown in Fig. 7. The storage time is defined as the time between the blue light being blocked and IR irradiation commencing. The solid lines are the least-square fits to the data points using the following equation:

$$n = n_o t^{-m}. \tag{12}$$

Figures 10 and 11 show the parameters for n_o and m as functions of temperature, respectively. The solid lines are fitted for temperatures in the range $200 \leqslant T \leqslant 400$ K as follows:

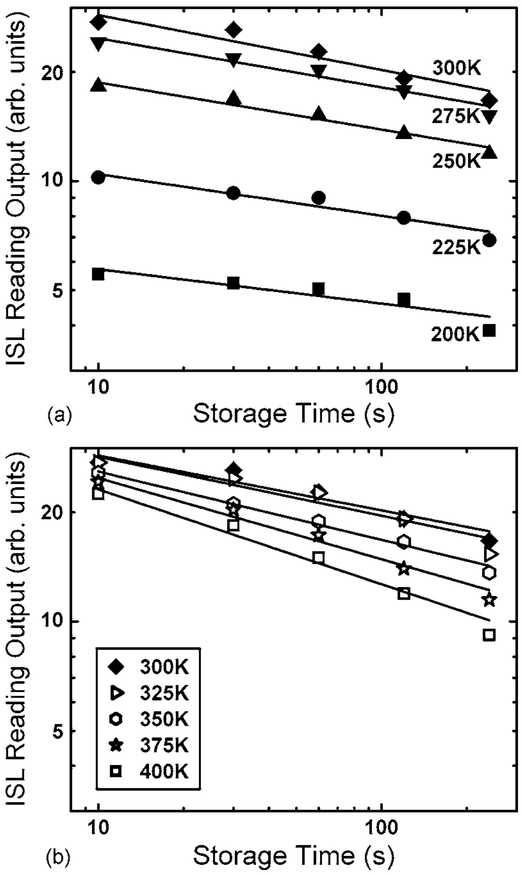

FIG. 9. ISL intensity versus storage time at different temperatures of IR stimulated emission at 650 nm. The solid lines are the least-square fitted to the data points.

$$n_o = \frac{43.2}{1 + 4.5 \times 10^{-5} \exp\left(\frac{2441.4}{T}\right)} \tag{13}$$

and

$$m = 0.095 - 6.4 \times 10^{-12}\ \mathrm{T}^4. \tag{14}$$

Here n_o is defined as the ISL reading output after a storage time of 1 sec and is mainly limited by writing efficiency as determined by the probability of electrons tunneling from Eu

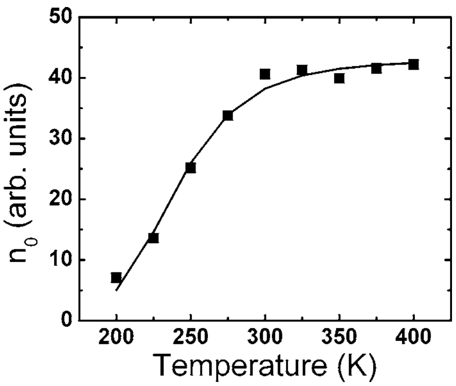

FIG. 10. n_o as a function of temperature. The solid line is a fit to the data points according to Eq. (13).

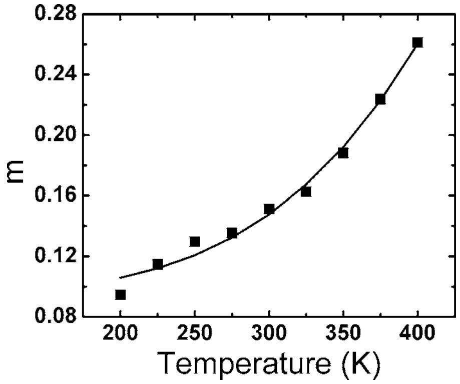

FIG. 11. m as a function of temperature. The solid line is a fit to the data points according to Eq. (14).

to Sm ions. At room temperature (300 K), m is found to be 0.16 for CaS:Eu,Sm. For comparison, a similar decay power law was used to fit ISL readout data taken at 300 K for both MgS:Eu,Sm and SrS:Eu,Sm yielding values for m of 0.21 and 0.16, respectively.[23] In the present study, we extended our analysis of the results for the value of m and its dependence on temperature. In Fig. 9, it is observed that for storage time ~10 sec, the ISL reading output increases with temperature and saturates at temperatures of 300 K and above. As discussed previously, this is due to the low writing efficiency at low temperature, which results in small reading output. With the increase of the storage time, the reading output decays follow the power law as fitted in Fig. 9. We observe that the decay rate at 200 K is so low that the reading output remains almost unchanged with storage time. On the other hand, the decay rate increases with temperature. This is mainly due to thermally assisted detrapping of Sm^{2+} trapped electrons.

Finally, the storage time of electrons in the CaS:Eu,Sm system can be estimated if in Fig. 7, we consider the minimum detectable signal for the ISL reading output to be twice the noise level within the range of 20 s. Thus, the estimated storage times for information written to CaS:Eu,Sm become 63 days at 300 K, 650 s at 400 K, and 363 s at 200 K. Note that the short storage time at 200 K is due mainly to the low writing efficiency at the low temperature. If the writing is done at a higher temperature such as 300 K and the sample is kept at 200 K, then the estimated storage becomes 388 866 days.

IV. CONCLUSION

The temperature dependence of PL and ISL in CaS:Eu,Sm is determined between 100 and 700 K. The data are analyzed using an electron-phonon-coupling model. It is shown that the quenching of the PL intensity can be fitted to two activation energies. The $\Delta E_1 = 0.55$ eV is due to some intervening quenching state while $\Delta E_2 = 0.056$ eV is attributed to the energy separation between the excited energy levels of Eu^{2+} ions and the conduction band of CaS. From the temperature dependence of ISL intensity, it is concluded that it is more efficient to write at higher rather than at lower temperatures, but reading efficiency is relatively not affected much by the effect of temperature. It is inferred that the lowest excited energy levels of Eu^{2+} ions is lower than that of Sm^{2+} ions by approximately $\Delta\varepsilon \sim 28$ meV. We further suggest that two different time constants are required to describe the depletion of electrons trapped at Sm centers under IR irradiation. Finally, studies of ISL reading output versus the storage time at different temperatures show that storage time is limited by thermally assisted detrapping of electrons from Sm^{2+} to Eu^{2+} ions.

---

*Email address: eleteokl@nus.edu.sg

[1] H. Nanto, Y. Douguchi, J. Nishishita, M. Kadota, N. Kashiwagi, T. Shinkawa, and S. Nasu, Jpn. J. Appl. Phys., Part 1 **36**, 421 (1997).

[2] Y. Tamura and A. Shibukawa, Jpn. J. Appl. Phys., Part 1 **32**, 3187 (1993).

[3] Y. Tamura, Jpn. J. Appl. Phys., Part 1 **33**, 4640 (1994).

[4] J. Lindmayer, Solid State Technol. **31**, 135 (1988).

[5] Y. Nakao, J. Phys. Soc. Jpn. **48**, 534 (1980).

[6] R. Carey, D. M. Newman, I. Viney, J. Wu, and J. Bickerton, J. Magn. Soc. Jpn. **25**, 248 (2001).

[7] F. Okamoto and K. Kato, J. Electrochem. Soc. **130**, 432 (1983).

[8] J. Gasiot, P. Braunlich, and J. P. Fillard, Appl. Phys. Lett. **40**, 376 (1982).

[9] K. Chakrabarti, V. K. Mathur, J. F. Rhodes, and R. J. Abbundi, J. Appl. Phys. **64**, 1363 (1988).

[10] K. Chakrabarti, V. K. Mathur, L. A. Thomas, and R. J. Abbundi, J. Appl. Phys. **65**, 2021 (1989).

[11] X. Sun, G. Hong, X. Dong, D. Xiao, G. Zhang, G. Tang, and W. Chen, J. Phys. Chem. Solids **62**, 807 (2001).

[12] G. Blasse, in *Handbook on the Physical Chemistry of Rare Earths*, edited by K. A. Gschneidner, Jr. and L. Eyring (North-Holland, Amsterdam, 1979), p. 237.

[13] K. Swiatek, M. Godlewski, L. Niinisto, and M. Leskela, J. Appl. Phys. **74**, 3442 (1993).

[14] K. Swiatek, K. Karpinska, M. Godlewski, L. Niinisto, and M. Leskela, J. Lumin. **60**, 923 (1994).

[15] N. Yamashita and S. Asano, J. Phys. Soc. Jpn. **56**, 352 (1987).

[16] M. Ando, Y. Abe, and Y. A. Ono, J. Appl. Phys. **70**, 5018 (1991).

[17] L. H. Robins and J. A. Tuchman, Phys. Rev. B **57**, 12094 (1998).

[18] C. Chen, K. L. Teo, T. C. Chong, Y. H. Wu, T. S. Low, R. Carey, D. M. Newman, I. Viney, J. P. Wu, and J. Bickerton, J. Appl. Phys. **93**, 2559 (2003).

[19] N. Singh and D. R. Vij, J. Mater. Sci. **29**, 4941 (1994).

[20] J. Rennie, E. Nakazawa, and T. Koda, Jpn. J. Appl. Phys., Part 1 **29**, 509 (1990).

[21] R. P. Rao, J. Lumin. **40**, 848 (1988).

[22] D. C. Morton, E. W. Forsythe, S. S. Sun, M. C. Wood, M. H. Ervin, and K. Kirchner, Appl. Phys. Lett. **78**, 1400 (2001).

[23] S. Albin, J. D. Satira, D. L. Livingston, and T. A. Shull, Jpn. J. Appl. Phys., Part 1 **31**, 715 (1992).

[24] Z. Hua, L. Salamanca-Riba, M. Wuttig, and P. K. Soltani, J. Opt.

Soc. Am. B **10**, 1464 (1993).

[25] S. Z. Hua, L. Salamanga-Riba, M. Wuttig, and P. K. Soltani, in *Semiconductor Heterostructures for Photonic and Electronic Applications*, edited by C. W. Tu, D. C. Houghton, and R. T. Tung, MRS Symposia Proceedings No. 281 (Materials Research Society, Pittsburgh, 1993), p. 597.

[26] H. Ruan, F. Gan, J. Xu, and Y. Chang, Mater. Sci. Eng., B **76**, 73 (2000).

[27] D. Jia, W. Jia, D. R. Evans, W. M. Dennis, H. Liu, J. Zhu, and W. M. Yen, J. Appl. Phys. **88**, 3402 (2000).

[28] Z. He, Y. Wang, L. Sun, Y. Hou, and X. Xu, Sci. China, Ser. A: Math., Phys., Astron. **44**, 1189 (2001).

[29] Z. He, Y. Wang, L. Sun, and X. Xu, J. Phys.: Condens. Matter **13**, 3665 (2001).

[30] J. Wu, D. Newman, and I. Viney, J. Lumin. **99**, 237 (2002).

[31] J. Wu, D. Newman, and I. Viney, J. Phys. D **35**, 968 (2002).

[32] J. Wu, D. Newman, and I. Viney, Appl. Phys. B **79**, 239 (2004).

[33] J. Wu, D. Newman, and I. Viney, J. Phys. D **37**, 1371 (2004).

[34] D. Curie, in *Optical Properties of Ions in Solids*, edited by B. DiBartolo (Plenum, New York, 1975), p. 71.

[35] T. Kobayashi, S. Mroczkowski, J. F. Owen, and L. H. Brixner, J. Lumin. **21**, 247 (1980).

[36] K. K. Rebane, in *Impurity Spectra of Solids: Elementary Theory of Vibrational Structure* (Plenum Press, New York, 1970) p. 253.